Colloids and Surfaces A: Physicochem. Eng. Aspects 522 (2017) 608–620

Contents lists available at ScienceDirect

Colloids and Surfaces A: Physicochemical and Engineering Aspects

journal homepage: www.elsevier.com/locate/colsurfa

Factors affecting the stability of water-oil-water emulsion films

N. Politova, S. Tcholakova*, N.D. Denkov

Department of Chemical and Pharmaceutical Engineering, Faculty of Chemistry and Pharmacy, Sofia University, 1 J. Bourchier Ave., 1164 Sofia, Bulgaria

HIGHLIGHTS

- The lifetime of oily films at concentrations up to 10 × CMC is equal to film drainage time.
- The oily films become stable only at concentrations higher than ca. 100 × CMC.
- At high surfactant and electrolyte concentrations the films remain thick for more than 1 h.
- The mass transfer of dissolved components explains the latter effect.
- No correlation between film stability and interfacial viscoelasticity is observed.

GRAPHICAL ABSTRACT

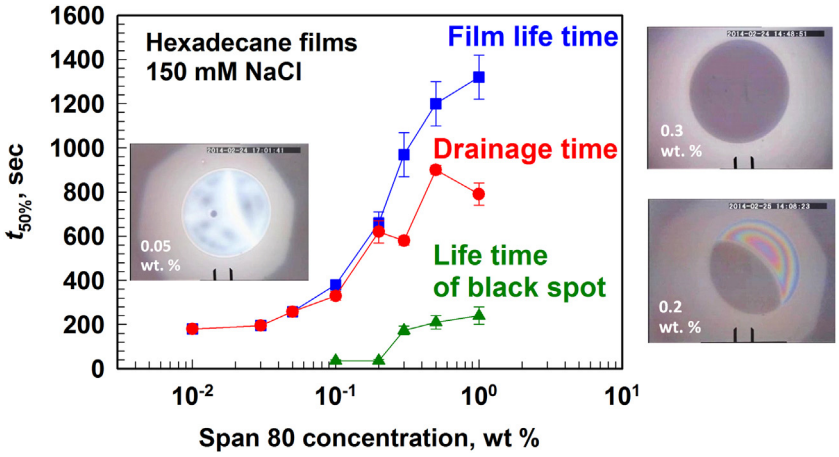

ARTICLE INFO

Article history:
Received 1 February 2017
Received in revised form 26 March 2017
Accepted 26 March 2017
Available online 29 March 2017

Keywords:
Oil film
Span 80
Adsorption
Water-in-oil emulsion
Capillary cell
Steric repulsion
Interfacial mass transfer

ABSTRACT

Water-oil-water (oily) liquid films appear between the droplets in water-in-oil emulsions. Here we report results from systematic experiments, aimed to clarify how several important factors affect the stability and drainage of such oily films, in the presence of the nonionic oil-soluble surfactant Span 80. These results reveal that: (1) At Span 80 concentrations around the CMC, the film lifetime coincides with the duration of film drainage. When the oily films reach a critical thickness of around 40 nm, unstable thinner black spots of thickness <10 nm are formed due to attractive van der Waals forces, and the films rupture within seconds; (2) At intermediate concentrations of 3–30 times the CMC, the films are again unstable, but their lifetime increases significantly with Span 80 concentration, due to a longer drainage time and higher stability of the formed thin black spots. The increased drainage time is explained with a faster surfactant adsorption which leads to lower interfacial tension and, hence, to lower capillary pressure driving the film thinning. (3) At even higher Span 80 concentrations (around and above 100 CMC) the drainage time approaches a constant value, ≈600 s. The films live much longer which is due mostly to the increased stability of the thin black films, formed after the black spot expansion. The

* Corresponding author.
E-mail addresses: SC@LCPE.UNI-SOFIA.BG, sc@dce.uni-sofia.bg (S. Tcholakova).

http://dx.doi.org/10.1016/j.colsurfa.2017.03.055

film drainage time at intermediate and high Span concentrations agrees very well with the theoretical predictions. Surprisingly, the addition of 500 mM NaCl into the aqueous phase leads to formation of non-equilibrium thick oil films, with drainage time >1 h. This effect is explained with a mass transfer of molecules between the aqueous and the oil phases which keeps the oil films out of equilibrium for a long period. These results can be used to explain and control the formation and stability of water-in-oil emulsions, in the presence of nonionic oil-soluble surfactants.

1. Introduction

The emulsion formation, stability and rheology are widely studied in relation to emulsion applications in petroleum industry, coating, food, cosmetics, pharmacy, and other technological areas [1–10]. In most of these studies, the researchers analyze the main factors affecting the stability of *oil-in-water* (O/W) emulsions during emulsification [5–8] and upon shelf-storage [9,10], as the emulsions of this type are most common in practice. The important role in emulsion stabilization of the van der Waals, electrostatic, steric (due to adsorbed polymers), depletion, capillary (due to adsorbed solid particles) and other types of surface forces has been revealed and explained [4,9,11–14]. In other studies, the formation of viscoelastic adsorption layers, e.g. by protein molecules and/or by protein-carbohydrate complexes, was shown to be important for emulsion stabilization, beside the surface forces acting in the emulsion films [15,16].

The stability of *water-in-oil* (W/O) emulsions has been also studied, due to the applications of these emulsions in food, cosmetic, chemical and petro-chemical industries [17–21]. It was shown, for example, that the stability of water-in-crude oil emulsions is related to the adsorption of asphaltenes and resins, originally present in the crude oil and acting as natural surfactants [22–24]. These surface active species form an adsorption layer at the oil-water interface with high surface visco-elasticity which can suppress the drop–drop coalescence [24–26]. Good correlation between the coalescence stability of water drops and the rheological response of the respective adsorption layers was established – the drops with fluid adsorption layers coalesce easily, whereas those with rigid layers are more stable [27,28].

The role of asphaltenes in the stability of model emulsion films of type water-oil-water was studied in detail by Tchoukov et al. [29] who found that asphaltenes form thicker adsorption layers, compared to bitumen and maltenes. The increased stability of asphaltene-containing films was attributed to the specific ability of the asphaltene molecules to self-assemble and form a 3D-network inside the emulsion films. This network structure stops the film drainage before the film could reach the critical thickness, at which it would rupture under the action of attractive surface forces [29]. In a similar consideration, the gelation of the continuous phase is used as an important mechanism for stabilization of many W/O emulsions in food and cosmetic industries [3]. In fact, several classes of food and cosmetic products (e.g. margarines and cosmetic creams) are W/O emulsions, trapped in a semi-solid state of their continuous phase.

The stability of liquid W/O emulsions, in which both the aqueous and the oil phases are in liquid state, is much less understood, as compared to the stability of W/O emulsions trapped in semi-solid state and of O/W emulsions. Liquid W/O emulsions are often encountered in chemical, petroleum, food and cosmetic industries, although there is a significant lack of understanding about the type of forces stabilizing these emulsions. It is generally known that some oil-soluble surfactants can ensure emulsion stability but the selection of these surfactants is still made by the method of trials-and-errors only, and the choice is relatively limited, as compared to the wide range of surfactants available for O/W emulsions.

One of the major difficulties for stabilization of the W/O emulsions is that the strong electrostatic repulsion, which is the main tool for stabilization of O/W emulsions (along with the steric repulsion by polymers), is not efficient for the reverse W/O emulsions. For example, in the pioneering work by Albers & Overbeek [30] a positive correlation was reported between the zeta-potential and the coalescence probability for water drops dispersed in benzene, which was explained with the higher mobility of the stabilizing molecules on the surface of the drops having higher zeta-potentials. In a more recent study Opawale & Burgess [31] compared the effect of Spans 20, 80, 83 and 85 on the water-in-mineral oil emulsions and tried to relate it to the rheological properties of the surfactant adsorption layers. It was shown that all surfactants form viscoelastic adsorption layers, except for Span 85. The effect of NaCl was also studied and it was found that the increase of NaCl concentration decreases the surface elasticity and reduces the stability of the respective emulsions.

In another study, lower sedimentation stability of W/O emulsions was determined in the presence of $MgSO_4$ in the aqueous phase [32]. This effect was attributed to the decreased rate of surfactant adsorption on the oil-water interface in the presence of $MgSO_4$. In a recent study Ushikubo & Cunha [33] compared the effect of three emulsifiers (PGPR, Span 80 and lecithin) on the stability of water-in-hexadecane and water-in-soybean oil emulsions. These authors proposed that the main stabilization mechanism against drop sedimentation is the steric stabilization by the surfactant tails. With respect to drop–drop coalescence, the authors proposed that the major factor is the viscoelasticity of the adsorption layers, formed on the drop surfaces. In addition, hydrodynamic interactions between the drops are also important for the drop stabilization and they could be enhanced by increasing the viscosity of the oily phase.

No information was provided in the aforementioned studies about the behavior and the stability of the oily emulsion films, formed between the colliding water drops, before their coalescence. The studies of emulsion film could provide important information about the mechanisms and the factors controlling the stability of the respective emulsions and about the role of the various components in the emulsion formulation [32,34,35].

Therefore, the major aim of the current study is to investigate the thinning behavior and the stability of oily films, formed from two alkane oils (hexadecane and Isopar V), in the presence of the oil-soluble surfactant Span 80, at different NaCl concentrations in the aqueous phase. Span 80 is chosen as this is one of the most widely used surfactants for stabilization of W/O emulsions in the chemical and food industries. The optical observations of the oily films are combined with characterization of the interfacial properties of the respective phases to explain the observed differences in the film drainage dynamics.

The paper is organized as follows: in Section 2 the used materials and methods are described; Section 3 presents Experimental results about the surface properties and the stability of the oily films; in Section 4 these results are analyzed to clarify the main

mechanisms of film stabilization; Section 5 describes the main conclusions from the performed work.

2. Materials and methods

2.1. Materials

As oily phase we used *n*-Hexadecane (95%, product of Alfa Aesar, cat. 43283) and Isopar V^{TM} (isoparaffin product of Exxon Mobil Corporation, product code: 133639) which have dynamic viscosities of 3 and 11 mPa.s, respectively. Isoparaffins are branched-chain alkanes with various technological applications. Both *n*-Hexadecane and Isopar V^{TM} oils were purified from surface-active contaminants by passing the oils through a glass column, filled with Florisil adsorbent (Supelco Florisil PR 60/100, product 20280-U) [36].

The surfactant sorbitane monooleate (Span 80, product of Fluka, cat. 85548, HLB ≈ 4.3) was dissolved in the oily phase via stirring on a magnetic stirrer at room temperature. The concentration of Span 80 was varied between 10^{-5} wt% and 1 wt%. In all cases, Span 80 dissolved completely in the oily phase and clear surfactant solutions were obtained. In all experiments we used water, purified by Milli-Q Organex system (Millipore Inc., USA) to prepare aqueous solutions of NaCl (≥99.8%, product of Sigma, cat.: 31434).

All studied concentrations of Span 80 are well below the onset of liquid crystal formation in the oily phase. To prove this statement we have performed additional experiments in which we determined the viscosity of the oily phases, as a function of Span 80 concentration. For all studied Span concentrations (up to 1 wt%) there is no any detectable increase in the viscosity of the oily phase (within ±0.1 mPa s). As an additional and decisive check we performed optical observations of the oily phase in cross-polarized light – we observed clear solutions without any indications for formation of liquid-crystalline domains.

To hydrophobize the glass capillary cell we used the vapors of Hexamethyldisilazane (HMDS, ≥99%, product of Aldrich, cat. 440191).

2.2. Interfacial tension

To measure the interfacial tension (IFT) on the water-oil interface we used Drop Shape Analysis with instrument DSA100R and software DSA1 (Krüss GmbH, Germany). The method consists of formation of a water drop, deformed by gravity, in the oily phase. The software automatically detects the drop profile and fits it by Laplace equation of capillarity to determine the interfacial tension as a function of time, $\sigma(t)$.

The interfacial dilatational rheological properties of the solutions were characterized by the oscillating drop method (ODM) [37]. The surface of the surfactant solution is perturbed sinusoidally, $a(t) = a_0 \sin(\omega t)$, where $a(t) = [A(t) - A_0]/A_0$ is the normalized change of the drop surface area around the mean area, A_0, while a_0 is the relative amplitude of oscillations. The resulting variation of surface tension is measured and (for small deformations) is presented as:

$$\sigma(t) = E_{SD} a_0 \sin(\omega t) + E_{ID} a_0 \cos(\omega t) \quad (1)$$

where E_{SD} is the surface storage modulus, related to surface dilatational elasticity, and E_{LD} is the surface loss modulus, related to surface dilatational viscosity, $\mu_{SD} = E_{LD}/\omega$. The total surface dilatational modulus is

$$E_D = (E_{SD}^2 + E_{LD}^2)^{1/2} \quad (2)$$

Measurements were performed at three frequencies of oscillations, between 0.1 and 0.5 Hz, the amplitude of deformation was between 3 and 5%, and at temperature $T = 25 \pm 1$ °C.

As shown by Alexandrov et al. [38] and by Stanimirova et al. [39] the transition from fluid to condensed visco-elastic adsorption layers can be detected as a substantial increase in the fit error, when describing the pendant-drop profile by the Laplace equation of capillarity. For all measurements included in the current manuscript, the fit error was always well below the threshold value that would indicate a transition from fluid to condensed adsorption layers. Therefore, we use the pendant drop method to determine the interfacial tension of the studied drops.

2.3. Observation of water-oil-water films in capillary cell

The oily films were formed and observed in reflected light in the capillary cell of Scheludko-Exerowa [40,41].The investigated oily phase solution is loaded in a cylindrical capillary, through an orifice in the capillary wall. Thus, a biconcave oily drop is formed inside the capillary. Then the water phase solution is poured in the cell to cover completely the oily drop. Next, the oily phase is sucked through the side orifice and the two oil-water menisci approach each other until a thin emulsion film is formed in the central part of the cell. By injecting or sucking liquid through the side orifice, one can vary the radius of the formed emulsion film. The inner radius of the used cell was $R = 1.5$ mm and the typical radius of the formed emulsion films is $R_F \approx 0.15$ mm.

To attach the oily film to the surface of the glass capillary, the latter was pre- hydrophobized by leaving it for 24 h in a tightly closed glass container, full of hexamethyldisylazane (HMDS) vapors.

2.4. Analysis of Span 80 composition

To determine the composition of Span 80 we used gas chromatography (GC). The analyses were performed on a TRACE GC apparatus (ThermoQuest, Italy) equipped with autosampler AS 2000. We used a capillary column Quadrex, USA, with the following specification: 5% phenyl methylpolysiloxane, 10 m length, I.D. 0.53 mm, 0.1 μm film thickness. Cold on-column injection was used, at a secondary cooling time of 0.3 min. The injection volume was 1 μL. The oven was programmed as follows: start at 45 °C, hold 1 min, ramp 1–230 °C at 5 °C/min, ramp 2–345 °C at 10 °C/min, hold 2 min. The flame-ionization detector (FID) temperature was set to 350 °C. The carrier gas was helium, set at a constant pressure flow mode (60 kPa). The detector gases were hydrogen and air, with nitrogen as make-up gas. The secondary cooling gas was nitrogen with a purity of 99.99%. All other gases were of 99.999% purity.

To determine Span 80 composition, it was first hydrolyzed by the following procedure, adapted from IUPAC [42]: First, we prepared 3.33 M alcoholic (80% ethanol) solution of potassium hydroxide (KOH). Then 0.22 g of Span 80 was weighted in a separate vessel and 3 mL of alc. KOH solution were added. The vessel was tightly closed and left for 4 h in a heating oven at 45 ± 5 °C. At every hour, the mixture in the vessel was homogenized by hand shaking. Afterwards, the obtained clear solution was left to evaporate in a vacuum dryer overnight. The next day, 24.5 mL of water were added to the vessel and the pH was lowered to 2 by addition of 5.5 mL 2 M HCl. The sample was then treated with 6 mL chloroform, and centrifuged. The chloroform extract was used for GC analysis.

Other samples without hydrolization were also analyzed. These experiments included GC analysis of 2 w/v% solution of Span 80 in chloroform.

Before injection, all the samples were derivatized by mixing with N,OBis(trimethylsilyl)trifluoroacetamide (BSTFA, derivatization grade, product of Supelco, product code: 33027) and pyridine (anhydrous, 99.8%, product of Sigma-Aldrich, product number: 270970) for 1 h at 60 °C.

The concentration of FA, mono-, di- and triesters was calculated using hexadecanol (cetanol) as internal standard.

3. Results and discussion

3.1. Interfacial tension isotherms

To characterize the solution surface properties, we measured the oil-water interfacial tension as a function of time, $\sigma(t)$, for Span 80 dissolved in purified hexadecane or Isopar V, see Fig. 1A. These data were fitted very well by an exponential function which shows that the adsorption is barrier-controlled [43]:

$$\sigma = \sigma_{EQ} + \Delta\sigma_1 \exp\left(-t/\tau_1\right) \quad (3)$$

Here σ_{EQ} is the equilibrium interfacial tension, while $\Delta\sigma_1$ is the initial interfacial stress which relaxes with a characteristic time τ_1. Illustrative experimental data for two concentrations of Span 80 in hexadecane and Isopar V are shown in Fig. 1A – one sees relatively good fits by Eq. (3) with regression coefficients $r^2 > 0.99$. This is also supported from the fact that the estimated characteristic diffusion time of Span 80 in hexadecane at 0.001 wt% is 22 s, whereas the characteristic time determined from our experimental data is 510 s, thus evidencing that the adsorption is barrier controlled in our systems.

For Span 80 concentrations below 0.01 wt%, the characteristic adsorption times for Isopar and hexadecane solutions are almost the same, whereas at Span 80 concentrations of 0.01 wt% and higher, the characteristic time τ_1 for hexadecane solutions is around 2-times shorter, as compared to that for the respective Isopar solutions, see for examples Fig. 1A. Most probably, the slower adsorption from Isopar solutions is due to a slower demicellization rate of the Span micelles in Isopar (compared to hexadecane), as the surfactant concentration at which we see this difference is around and above the critical micellization concentration, CMC (cf. Fig. 1B). Other possible explanation is that the transfer of surfactant molecules from oily to water phase depends on the oily viscosity and that is why we measure longer relaxation time for more viscous oil.

From the best fit to the experimental data we determined the equilibrium interfacial tension at given surfactant concentration, $\sigma_{EQ}(C_S)$ – see Fig. 1B. The CMC of Span 80 is ≈0.01 wt% in Isopar V, whereas in hexadecane CMC ≈ 0.007 wt%. The interfacial tension at CMC is $\sigma_{CMC} \approx 2.5$ mN/m for hexadecane-water and $\sigma_{CMC} \approx 2.7$ mN/m for Isopar V-water. These very similar values show that the presence of branched alkane molecules in Isopar does not affect strongly the structure and properties of Span 80 adsorption layers. At $C_S <$ CMC, the interfacial tension for Isopar-water interface is slightly higher at the same surfactant concentraton, by ca. 5 mN/m, as compared to hexadecane-water interface.

To determine the characteristic parameters of the adsorption layers on hexadecane-water and Isopar-water interfaces, we fitted the experimental data $\sigma_{EQ}(C_S)$ by Volmer adsorption isotherm which implies non-localized adsorption with negligible interaction between the adsorbed molecules [43,44]

$$K_A C_S = \frac{\Gamma}{\Gamma_\infty - \Gamma} \exp\left(\frac{\Gamma}{\Gamma_\infty - \Gamma}\right) \quad (4a)$$

$$\sigma_e = \sigma_0 - kT\Gamma_\infty \left(\frac{\Gamma}{\Gamma_\infty - \Gamma}\right) \quad (4b)$$

Here K_A is the adsorption constant, σ_0 is the surface tension of the pure interface ($\sigma_0 = 52.8 \pm 0.2$ mN/m for hexadecane-water and Isopar-water interfaces at 20 °C) and $\Gamma\infty$ is the maximum surfactant adsorption in the adsorption monolayer. From the values of K_A and Γ_∞ we calculated the adsorption at CMC using Eqs. (4a) and (4b), see Table 1. From the value of K_A we determined also the adsorption energy of the Span 80 molecules using the relation [43]:

$$K_A = \frac{\delta}{\Gamma_\infty} e^{\frac{\Delta\mu}{kT}} \quad (5)$$

Here $\delta \approx 2.0$ nm is the thickness of the adsorption layer which was approximated with the length of the adsorbed molecules; $\Delta\mu$ is the standard free energy of adsorption (the energy gain of bringing a molecule from the bulk solution to the interface). The description of the experimental data by Volmer equation is shown as continuous curves in Fig. 1B and the characteristic parameters of the respective adsorption layers are listed in Table 1.

The values of the area-per-molecule at CMC, A_{CMC}, are in a qualitative agreement with those published in literature. Peltonen et al. [45] studied Span 80 adsorption on alkane-water interfaces for alkanes with different chain-lengths, varied between pentane and dodecane. These authors showed that the surface area decreases from 0.46 to 0.37 nm^2 while increasing the alkane chain-length. The smaller surface area, determined in our current work, $A_{CMC} \approx 0.30$ nm^2, is probably due to the longer chain-length of hexadecane, used in our study. Opawale & Burgess [46] studied Span 80 adsorption on light mineral oil-water interface and determined an area-per-molecule of 0.32 nm^2, which is very close to the values determined by us. There is no significant difference in A_{CMC} for the adsorption layers formed on hexadecane-water and Isopar-water interfaces.

The adsorption energy is somewhat lower for Isopar-water interface, as compared to hexadecane-water interface which is in a good agreement with the observed higher CMC for Isopar. The relatively high adsorption energies determined, 12.5–14 kT, can be explained with the formation of strong and energetically favored hydrogen bonds between the sorbitan ring of the adsorbed Span molecules and the water molecules at the interface. The measured adsorption energies are also in a reasonable agreement with literature data, as 15.5 kT was reported for dodecane-water interface [45].

To check for the effect of NaCl on the interfacial properties, we measured Span 80 adsorption isotherms for hexadecane-water interface, with the aqueous phase containing 0, 150 or 500 mM NaCl. One sees from Fig. 2A that the kinetics of Span 80 adsorption on hexadecane-water interface does not depend significantly on the presence of NaCl in the aqueous phase. On the other hand, the equilibrium interfacial tension is slightly lower for the solutions without NaCl at $C_S <$ CMC and slightly higher for the solutions with $C_S >$ CMC.

3.2. Interfacial rheological properties of the solutions studied

To characterize further the adsorption layers, formed on hexadecane-water interface, we measured their surface dilatational modulus at three Span 80 concentrations higher than CMC. The obtained results are shown in Fig. 3. The surface elastic modulus is the highest at the lowest surfactant concentration studied, 0.01 wt%, and reaches 50 mN/m at high oscillation frequency. The increase of Span concentration leads to much lower surface modulus which becomes around several mN/m at 0.1 wt% and ≈1 mN/m at 1 wt% Span 80. This reduction in the surface modulus is due to the faster surfactant adsorption at higher concentrations, so that the surface tension remains very close to the equilibrium one upon drop surface deformation.

The effect of NaCl on the rheological properties of the adsorption layers was also studied but no any significant effect was detected, see Fig. 3B.

From this series of experiments we conclude that Span 80 forms dense adsorption layers with relatively small area-per-molecule at both hexadecane-water and Isopar-water interfaces. The charac-

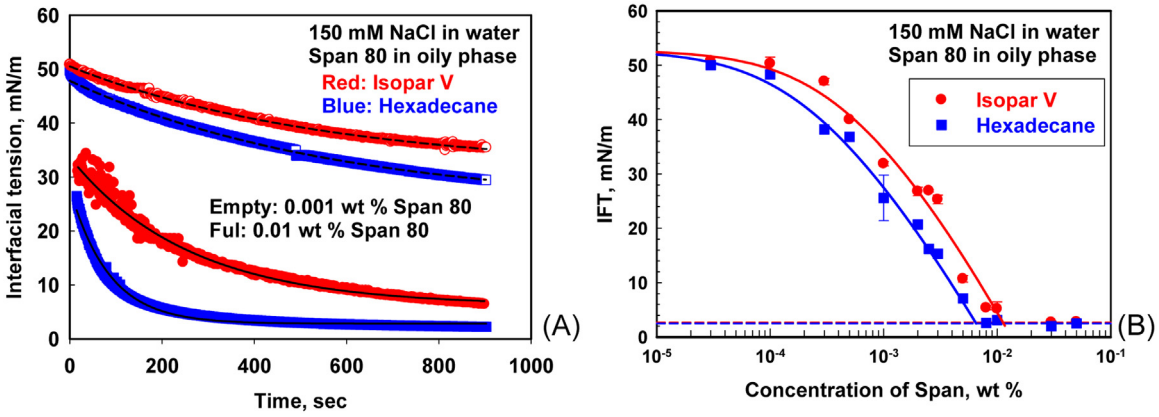

Fig. 1. (A) Interfacial tension as a function of time for 0.001 wt% (empty points) and 0.01 wt% (full points) Span 80 solutions in Isopar V (red circles) and Hexadecane (blue squares) along with the best fits according to Eq. (3). (B) Equilibrium interfacial tension as a function of Span 80 concentration in Isopar V (red circles) and Hexadecane (blue squares). The curves in (B) are fits by Volmer adsorption isotherm, Eq. (4). The aqueous phase contains 150 mM NaCl. (For interpretation of the references to colour in this figure legend, the reader is referred to the web version of this article.)

Table 1
Adsorption constant, K_A, adsorption energy, $\Delta\mu/k_BT$, maximal adsorption, Γ_∞, critical micellar concentration, CMC, area per molecule in the adsorption layer at CMC, A_{CMC}, and surface coverage at CMC, $\theta_{CMC} = \Gamma_{CMC}/\Gamma_\infty$. The reported values in the table correspond to the total surfactant adsorption on the surface.

Oily phase	NaCl, mM	K_A, m^3/mol	$\Delta\mu/kT$	Γ_∞, μmol/m^2	CMC,newline wt%	A_{CMC}, Å^2	θ_{CMC}
Hexadecane	0	430 ± 100	14.0 ± 0.3	6.8 ± 0.8	0.0065	33 ± 3	0.75
	150	170 ± 40	13.3 ± 0.3	8.4 ± 0.8	0.0065	29 ± 3	0.71
	500	290 ± 60	13.6 ± 0.3	6.7 ± 0.8	0.0095	33 ± 3	0.75
Isopar V	150	77 ± 40	12.5 ± 0.7	8.9 ± 1.6	0.01	28 ± 5	0.69

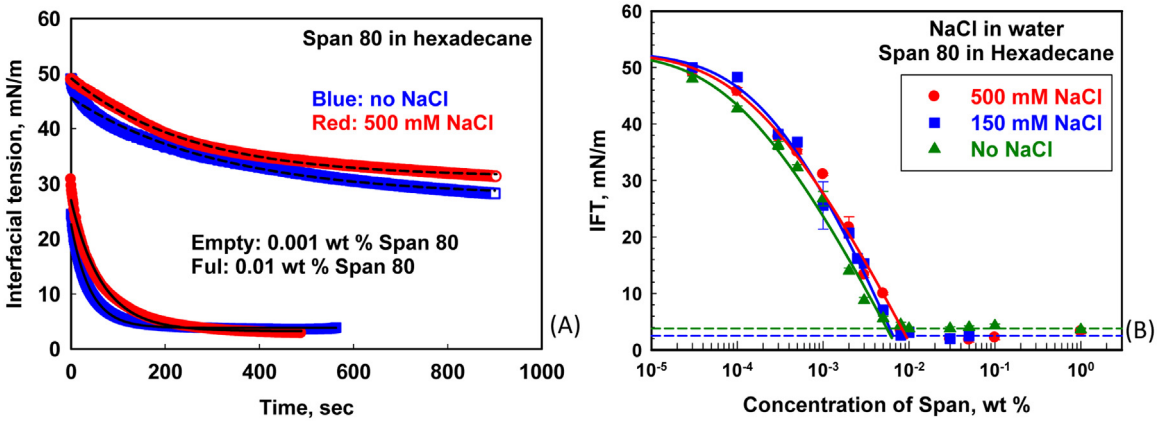

Fig. 2. (A) Interfacial tension as a function of time for 0.001 wt% (empty points) and 0.01 wt% (full points) Span 80 solutions in hexadecane without (blue squares) and with 500 mM NaCl (red symbols) in the water phase, along with the best fits by Eq. (3). (B) Equilibrium interfacial tension, as a function of Span 80 concentration in hexadecane, when the water phase contains no NaCl (green triangles), 150 mM NaCl (blue squares) or 500 mM NaCl (red circles). (For interpretation of the references to colour in this figure legend, the reader is referred to the web version of this article.)

teristic adsorption time is almost the same for both interfaces at $C_S < CMC$, while it is around twice shorter for hexadecane-water interface at $C_S \geq CMC$. The apparent interfacial elasticity and viscosity, measured upon interfacial oscillations, decrease significantly with increasing C_S and becomes ≈1 mN/m at 1 wt% Span 80. The latter effect is due to the faster kinetics of adsorption at this concentration. No significant effect of NaCl on the properties of adsorption layers is observed.

3.3. *Lifetime of hexadecane films, formed between 150 mM aqueous solutions of NaCl*

Here we summarize the results about the stability of 350 ± 50 μm in diameter hexadecane films, sandwiched between two 150 mM aqueous solutions of NaCl. At least 10 films for each Span 80 concentrations were observed to acquire sufficient statistical information, as the film rupture is a stochastic process.

The initially formed films had inhomogeneous thickness. Thicker region (dimple) is formed first in the film center. Most of the liquid in the dimple rapidly leaves the film, within 2–5 s after film formation, while part of the dimple remains captured in the film as shown in Fig. 4A. Even 2 min after its formation, the film still bears some remnant structure of the initial dimple – about one-third of the film has thickness >100 nm (left side in Fig. 4B), while the rest has thickness ≈70 nm. Further gradual thinning is observed and, after certain period of time which depends significantly on the concentration of Span 80, a black spot with thickness <10 nm is formed in the thinnest part of the film, see Fig. 4C. Depending on the Span concentration, this black spot can expand in diameter without film

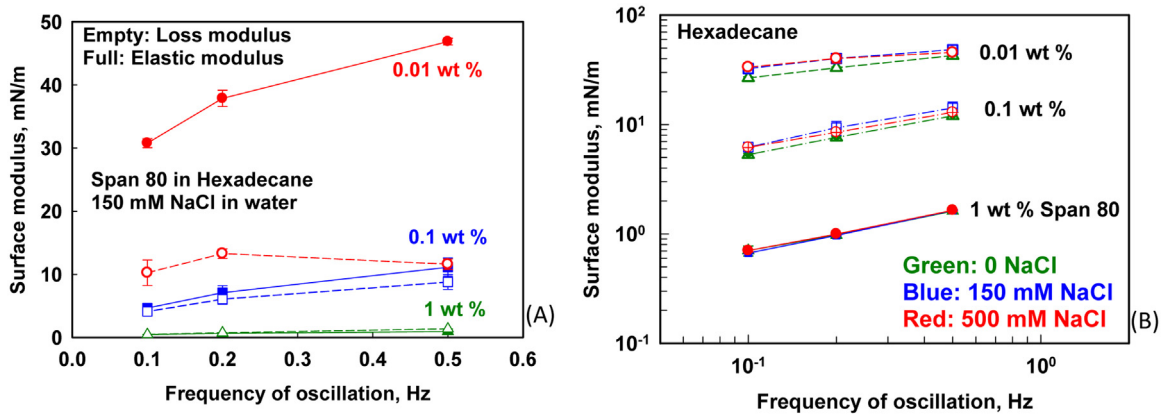

Fig. 3. Surface modulus as a function of frequency of oscillation for adsorption layers formed on hexadecane-water interface from 0.01 wt% (red circles); 0.1 wt% (blue squares) and 1 wt% (green triangles) Span 80 oily solutions at (A) 150 mM NaCl and (B) at three different NaCl concentrations in the aqueous phase. (For interpretation of the references to colour in this figure legend, the reader is referred to the web version of this article.)

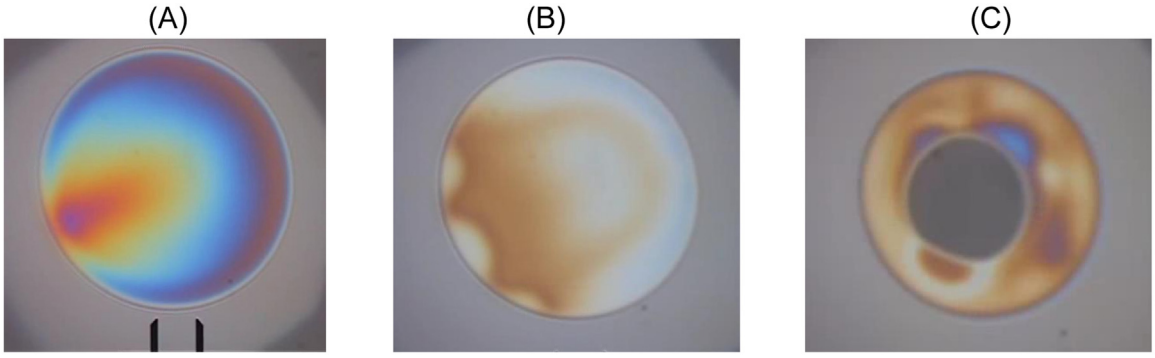

Fig. 4. Typical images of thinning hexadecane film, stabilized by 0.1 wt% Span 80 at different stages: (A) 30 s after film formation; (B) 2 min later, and (C) just before film rupture.

rupture or the film ruptures during the spot expansion (which is the case with the film shown in Fig. 4).

At the lowest Span 80 concentration of 0.01 wt.%, the film lifetime is determined entirely by the drainage time of the film from its initial thickness to the critical film thickness, $h_{CR} \approx 45 \pm 5$ nm, at which the black spot appears, due to van der Waals attraction between the film surfaces. At this low surfactant concentration, the films rupture almost immediately after black spot formation, see Fig. 5A. The increase of Span concentration in the hexadecane leads to significant increase in both the drainage time (until the black spot is formed) and in the time required for film rupture after the black spot formation. At concentrations above 0.3 wt.%, the black spot expands until it occupies the entire film area (Fig. 5D). These films rupture much later and some of them remain stable for more than 30 min.

To characterize quantitatively the stability of these films, we determined the probability for film rupture as a function of the film lifetime, for different Span 80 concentrations, see Fig. 6. One sees that the probability for film rupture increases significantly with time, for all studied Span concentrations, and becomes 100% within 200–1000 s for $C_S \leq 0.2$ wt%. At higher Span 80 concentration, some fraction of the films remains stable even after 2000 s of observation. This fraction of stable films increases with the increase of Span 80 concentration. Note that all concentrations shown in Fig. 6 are around and above the CMC. Nevertheless, most of the films are unstable even at the highest concentration studied, $C_S = 1$ wt%, and a significant increase in the film stability is observed with the increase of surfactant concentration.

To gain further information about the mechanisms of film stabilization and film rupture, we measured also the probability for film rupture after black spot formation. For $C_S \leq 0.05$ wt%, the probability for film rupture is 100% within 1 s after the black spot formation, see Fig. 6B. However, at higher surfactant concentrations this probability decreases. In other words, the stability of the final equilibrium films with thickness <10 nm increases significantly with the increase of Span 80 concentration. The threshold surfactant concentration, at which the black spot can expand and cover the entire film area, is 0.3 wt% (viz. 30 times CMC). At lower Span concentrations, the film ruptures immediately after the formation or during the expansion of the black spot, whereas at higher Span concentration about 50% of the thin black films live, at least, for 3–5 min after the black spot formation.

To characterize further the effect of Span 80 concentration on the film stability, we define three characteristic times: the average lifetime of the film, τ_L, which is defined as the time at which 50% of all studied films rupture; the average film drainage time, τ_{DR}, which is defined as the time required for formation of a black spot inside 50% of the observed films; and the average lifetime of the black spot, τ_S, which is defined as the time for which 50% of the films will rupture after the formation of the black spot. Note that $\tau_L = (\tau_{DR} + \tau_S)$ by definition.

The experimental results for these three characteristic times are compared in Fig. 7, as functions of Span 80 concentration. From these data we conclude that, depending on Span concentration, we may distinguish three regions. At $C_S \leq 0.05$ wt% the lifetime of the films is controlled entirely by their drainage time, $\tau_L \approx \tau_{DR}$. The appearance of a black spot in these films leads to a film rupture

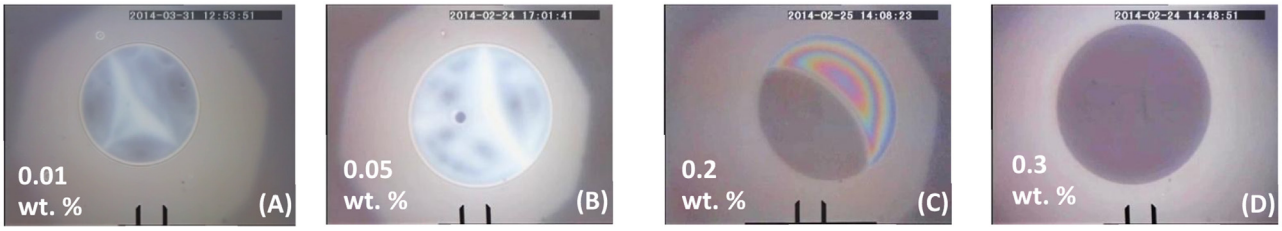

Fig. 5. Images of hexadecane films, stabilized by Span 80 of different concentrations (indicated on the images), just before film rupture. The aqueous phase contains 150 mM NaCl. The distance between the dark vertical bars is 50 μm.

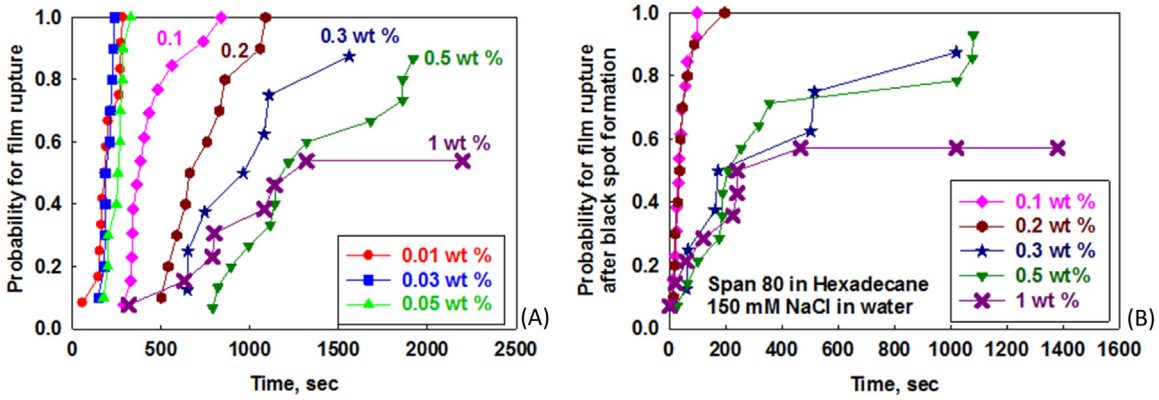

Fig. 6. Probability for film rupture (A) after its formation and (B) after black spot formation, as a function of time, for hexadecane films stabilized with Span 80 of different concentrations, as indicated in the figures. The aqueous phase contains 150 mM NaCl.

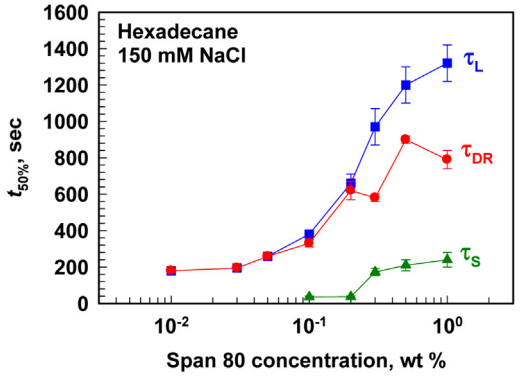

Fig. 7. Time required for 50% of films to break after their formation, τ_L, to break after black spot formation, τ_S, and to drain to thickness at which the black spot is formed, τ_{DR}, as a function of Span 80 concentration in hexadecane. The aqueous phase contains 150 mM NaCl.

within 1 s after spot formation. In the intermediate concentration range, 0.1 wt% ≤ C_S ≤ 0.2 wt%, the film lifetime increases mainly due to increase of the drainage time, while the lifetime of the black spots is still short and they survive for ≈30 s. Further increase to C_S ≥ 0.3 wt% does not change significantly τ_{DR}, but both τ_L and τ_S increase significantly – about 50% of the thin films remain stable for more than 1400 s at the highest surfactant concentrations, due to the increased lifetime of the black films.

From these results we conclude that the stability of the hexadecane films is rather low, even at concentrations much higher than CMC. The films formed from Span 80 solutions with C_S ≤ 0.05 wt% rupture immediately after the formation of a black spot with thickness <10 nm which happens at a critical film thickness $h_{CR} \approx 45 \pm 5$ nm for less than 300 s after the film formation. The films formed from Span 80 solutions with 0.1 wt% ≤ C_S ≤ 1 wt% have much longer drainage time (between 500 and 1100 s) before the formation of a black spot inside the film. This is the main effect which leads to increased lifetime of the films, formed from solutions with the intermediate concentration 0.1 ≤ C_S ≤ 0.2 wt% Span 80. The further increase in the surfactant concentration leads not only to longer drainage time, but also to significant increase in the stability of the thin films with thickness below 10 nm. All these trends are discussed in Section 4 below.

3.4. Role of the oily phase for the stability of water-oil-water films

Similar series of experiments was performed with Span 80 solutions in Isopar V. The experimental results for the three characteristic times, τ_L, τ_{DR} and τ_S, are shown in Fig. 8. One sees that the stability of the Isopar films is similar to that of the hexadecane films at C_S ≤ 0.03 wt%. The further increase of Span 80 concentration in Isopar leads to significant increase in τ_{DR} and, as a consequence, the stability of the Isopar films becomes much higher as compared to hexadecane films. At the highest Span 80 concentration, all studied films are stable for more than 2 h. The drainage time is very long, but even after the black spot formation, all films remains stable for more than 20 min. Therefore, the much higher stability of Isopar films, at high surfactant concentration, is related to both longer drainage time and higher stability of the thin film. Interestingly, we observed that the longer drainage time is related to very slow drainage of the central part of the film, whereas the periphery remains thicker which might be an indication for non-equilibrium processes, like those discussed for hexadecane films in Section 4 below.

From this series of experiments we conclude that the stability of the films, formed from Span 80 solutions in hexadecane and Isopar V, is almost the same at $C_S \approx$ CMC, whereas both τ_{DR} and τ_L increase more rapidly at $C_S \geq 3$ times CMC, when Isopar is used as oily phase. On the other hand, the shapes of the curves for τ_{DR}, τ_S and τ_L are qualitatively (in shape) very similar for hexadecane and Isopar.

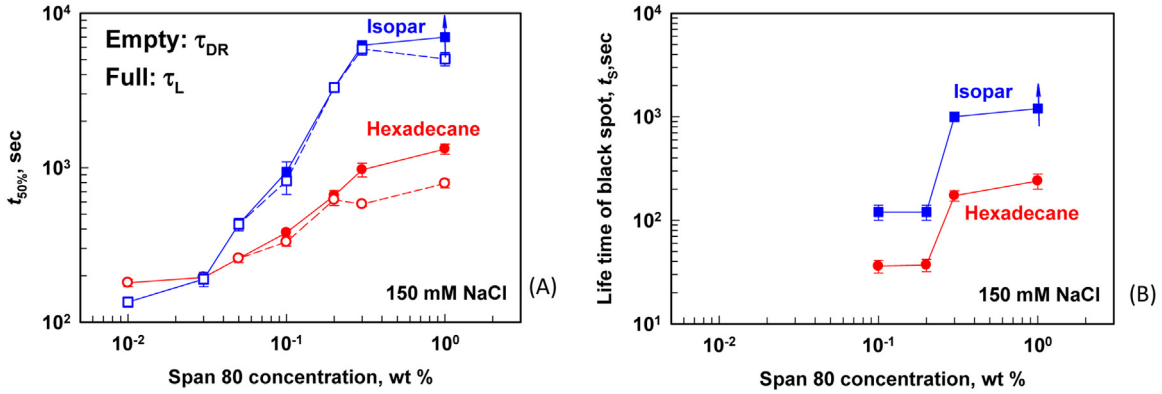

Fig. 8. (A) Drainage time (empty points) and life time (full points) and (B) Life time of black spot as a function of Span 80 concentration in Hexadecane (red circles) and in Isopar (blue squares). Water phase contains 150 mM NaCl. (For interpretation of the references to colour in this figure legend, the reader is referred to the web version of this article.)

3.5. Role of NaCl in the aqueous phase for water-hexadecane-water films

To study the effect of electrolyte concentration in the aqueous phase, we performed experiments with hexadecane films containing 0.01, 0.1 or 1 wt% Span 80, sandwiched between aqueous phases, containing 0, 150 or 500 mM NaCl.

At the lowest Span concentration of 0.01 wt%, the behavior of the films, formed between NaCl solutions of different concentrations was very similar. The drainage time to ≈100 nm thickness was relatively short. Afterwards, the films drained to ≈45 nm, when a black spot was formed and the films ruptured. As a consequence, $\tau_L \approx \tau_{DR}$ for these films. The presence of NaCl in the aqueous phase slightly accelerated the film thinning and τ_L decreased from ≈200 s to ≈155 s with increasing NaCl concentration in the aqueous phase, see Fig. 9A. Therefore, the addition of NaCl to the aqueous phase does not affect significantly the lifetime of the oily films at low Span 80 concentration.

At intermediate concentration of 0.1 wt% Span, τ_{DR} varies between 200 and 1200 s. This time is much longer for films formed in aqueous phase without NaCl and 500 mM NaCl, while it is much shorter for solutions containing 150 mM NaCl. Therefore, τ_{DR} passes through a minimum at C_{EL} = 150 mM. The results for the probability for rupture of the thin films are shown in Fig. 9C. One sees that the film ruptures ≈100 s after the black spot formation, for films formed in solutions with 150 and 500 mM NaCl, whereas some of the films remain very stable, when water without NaCl is used. Therefore at this concentration of Span 80, the stability of the thin films is higher when no NaCl is present in the aqueous phase. The mechanistic explanation of these noticeable effects of NaCl on the lifetime and the drainage time of oily films, stabilized by nonionic surfactant, are not very clear at the moment. They probably include a contribution of non-equilibrium mass-transfer effects, like those discussed in Section 4.

Experiments with 1 wt% Span 80 were also performed. At this concentration, we could not observe the oily films formed in water without NaCl, because no film could be formed in the capillary cell – upon attempts to form a film, the oil immediately detached from the capillary in the form of oily drops. Rather unexpected behavior was observed for the hexadecane films, formed between 500 mM NaCl solutions. More than 80% of the formed films remained thicker than 100 nm up to 1 h after their formation, see Fig. 10. In less than 20% of the films, we observed the formation of a black spot which remained stable for more than 15 min. Therefore, the films formed from 1 wt% Span 80, between 500 mM NaCl solutions, are very stable. Note that the stability of the films formed between 150 mM NaCl solutions, is much lower. Only 50% of them remained stable after the black spot formation and τ_{DR} is ≈12 min only.

From this series of experiments we can conclude that the presence of NaCl in the aqueous phase affects slightly the stability of films formed at 0.01 wt% Span 80 concentration. The drainage time passes through minimum at 150 mM NaCl for films formed at 0.1 wt% Span 80 in the hexadecane. Much shorter drainage time is determined for films formed from 1 wt% Span 80, in the presence of 150 mM NaCl, as compared to 500 mM NaCl.

4. Discussion

The experimental results presented in Section 3 can be summarized as follows:

(1) At low Span 80 concentrations, $C_S \leq 0.03$ wt%, the formed films rupture immediately after black spot formation, viz. $\tau_L \approx \tau_{DR} \approx 200$ s. The drainage time does not depend significantly on the surfactant concentration in the oil phase, NaCl concentration in the aqueous phase, or oil viscosity.
(2) At intermediate surfactant concentrations, 0.05 wt% $\leq C_S \leq$ 0.2 wt%, the oil films rupture during the black spot expansion. In this concentration range, τ_{DR} increases with C_S and with oil viscosity, while it passes through a minimum at 150 mM NaCl when the electrolyte concentration is varied between 0 and 500 mM. The lifetime of the thin film, τ_S, depends on the surfactant concentration and the oil type, whereas it does not depend significantly on NaCl concentration.
(3) At high surfactant concentrations $C_S \geq 0.3$ wt%, the oil films rupture after the formation of a thin film with thickness ≈10 nm. In this concentration range, τ_{DR} does not depend on Span concentration, but it depends on the oil type and on NaCl concentration in the aqueous phase. The lifetime of the thin films, τ_S, depends on C_S, NaCl concentration and oil type.

Comparing these trends with the results for the surface modulus of the adsorption layers, presented in Section 3.1, we see that the oil film stability is definitely not controlled by the rheological properties of the adsorption layers. Indeed, the higher surfactant concentration leads to lower surface moduli, whereas the stability of the oily films increases with increasing the surfactant concentration. Thus, anti-correlation is observed between the film lifetime and the surface modulus, due to the fact that the adsorption is much faster at higher surfactant concentration and, hence, the surface modulus decreases, while the stability of the oily film increases

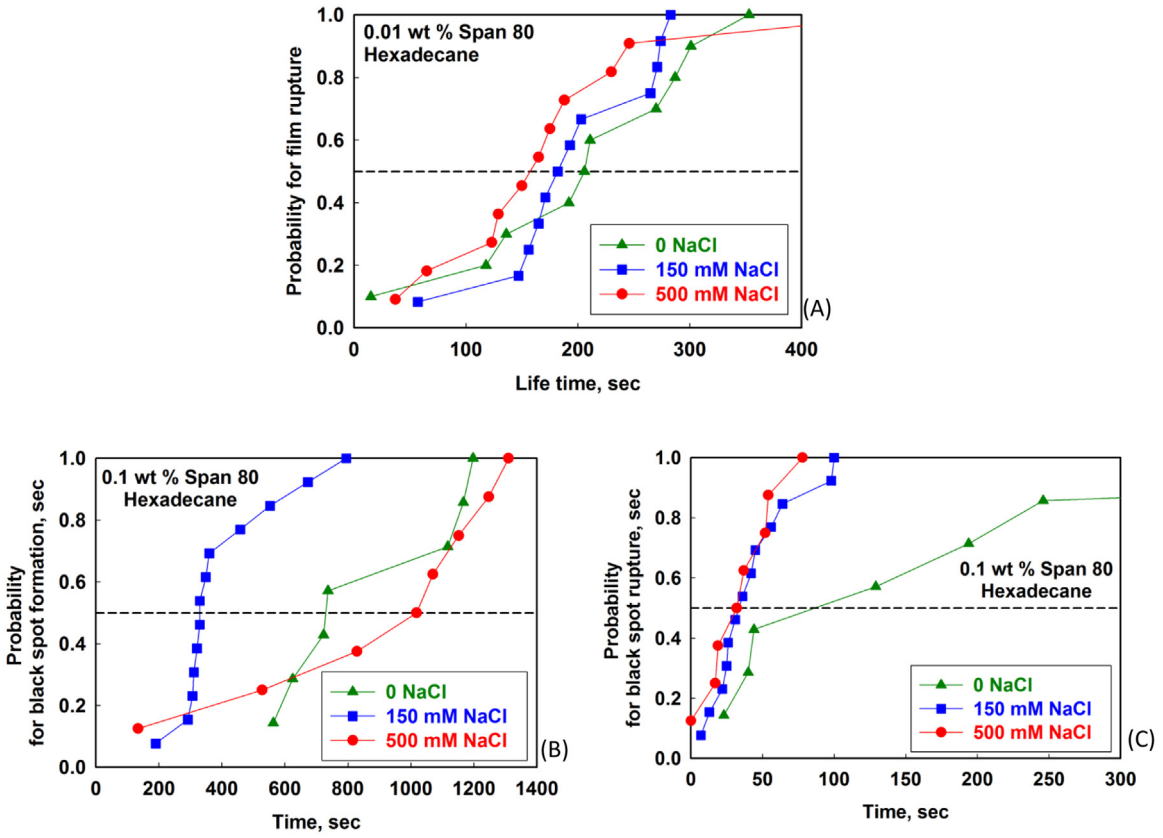

Fig. 9. (A) Probability for film rupture of films stabilized by 0.01 wt% Span 80; (B) Probability for black spot formation and (C) Lifetime of black spots for films stabilized by 0.1 wt% Span 80. The aqueous phases contain 0, 150 or 500 mM NaCl as indicated in the figures.

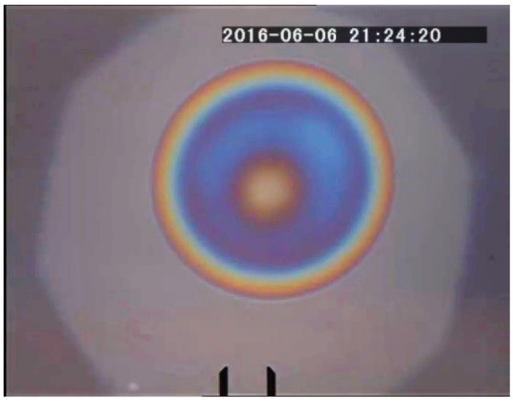

Fig. 10. Hexadecane film, stabilized with 1 wt% Span 80, and formed between two aqueous phases, containing 500 mM NaCl. The picture is taken 1 h after the film formation and the colored reflected light indicates film thickness which is ≥300 nm.

(the same is true for the stability of the actual emulsions, stabilized by Span 80).

Because the film stability in the first concentration range, $C_S \leq 0.03$ wt%, is controlled by the film drainage time, τ_{DR}, until reaching the critical film thickness, h_{CR}, we estimated τ_{DR} using theoretical models available in the literature. Since the studied films are with uneven thicknesses, we use the equation proposed by Manev, Tsekov & Radoev (MTR) [47] which accounts for the non-homogeneous thickness on the rate of film thinning:

$$V_{MTR} = -\frac{dh}{dt} = \frac{8}{3\eta}\sqrt[5]{\frac{4h^{12}P_C^8}{\alpha_1^{12}\sigma^3 R_F^4}} \quad (6)$$

Here V_{MTR} is the rate of film thinning, h is the average instantaneous film thickness, t is time, η is the viscosity of the liquid in the film, σ is the interfacial tension, R_F is the film radius, $\alpha_1 = 3.8317$ is the first root of the first order Bessel function of first kind, and P_C is the capillary pressure which can be determined by the equation [48]:

$$P_c = \frac{2\sigma R_C}{R_C^2 - R_F^2\cos\psi} \approx \frac{2\sigma}{R_C} \quad (7)$$

where $R_C = 1.5$ mm denotes the radius of the capillary cell, $R_F \approx 150$ μm is the film radius and $\psi < 1^\circ$ is the contact angle film-meniscus. As far as R_C is 10-times larger than R_F, we neglect the second term in the denominator and use the approximate equation (7).

Integration of Eq. (6), along with Eq. (7), leads to the following explicit expression for the drainage time from an initial thickness h_0 to the critical film thickness h_{CR}:

$$\tau_{MCR} = \frac{15\eta}{224\sigma}\sqrt[5]{\alpha_1^{12}R_C^8R_F^4}\left(\frac{1}{h_{CR}^{7/5}} - \frac{1}{h_0^{7/5}}\right) \quad (8)$$

The above equation implies that, at fixed interfacial tension, the drainage time should be proportional to the oil viscosity, 3 mPa s for hexadecane and 11 mPa s for Isopar V. However, at $C_S \leq 0.03$ wt% we did not measure experimentally a longer drainage time for the more viscous Isopar V oil, see Fig. 8A. On the other hand, in this concentration range, the surfactant adsorption is much slower for Isopar V as compared to hexadecane, see Fig. 1A. Furthermore, since the surface tension decrease is comparable with the drainage time of the oily films, see Fig. 1A, we have to account for the non-equilibrium surface tension (which is higher than the equilibrium one) during the process of film thinning. Instead of constant interfacial tension, we have substituted Eq. (3) into Eq. (8) and thus we have derived

the following transcendental equation for the drainage time of films with inhomogeneous film thickness and decreasing interfacial tension along the process of film drainage:

$$\tau_{MCR}\sigma_{EQ} + \Delta\sigma_1\tau_1\left(1-\exp\left(-\tau_{MCR}/\tau_1\right)\right) = \frac{15\eta}{224}\sqrt[5]{\alpha_1^{12}R_C^8R_F^4}\left(\frac{1}{h_{CR}^{7/5}}-\frac{1}{h_0^{7/5}}\right) \quad (9)$$

Here σ_{EQ}, $\Delta\sigma_1$ and τ_1 are all parameters, determined in the surface tension measurements. Using Eq. (9) we estimate that the drainage time for hexadecane films at 0 mM NaCl should be ≈280 s, whereas for 500 mM NaCl it should be ≈150 s, which is in a reasonably good agreement with the experimentally determined values of 210 s for 0 mM NaCl and 156 s for 500 mM NaCl. The calculated value of the drainage time for Isopar V films at 0.01 wt% Span 80 is ≈180 s, which is again very close to the experimental value of ≈160 s. Therefore, the small variations in the drainage time at low surfactant concentrations are related to the different kinetics of surfactant adsorption, which leads to different capillary pressures driving the film drainage. It should be mentioned that there could be some depletion of surfactant in the film interior, especially at low surfactant concentrations. However, in the real systems the surfactant adsorption occurs not only during the film thinning, but also before the emulsion film is formed and inside the meniscus region surrounding the film while the film is thinning. Therefore, we could expect that the film surface tension is similar (though not exactly the same) to the one measured with single interfaces. The good agreement between the drainage times, estimated above using this assumption, and the experimental drainage times support our approach.

From these estimates we conclude that, at low surfactant concentrations (up to 3-times CMC), the lifetime of the oily films coincides with the time for film drainage to the critical film thickness h_{CR}. The film drainage is much faster, as compared to the predictions of Reynolds equation, because the films have inhomogeneous thickness [47] and the interfacial tension of the film surfaces is higher than the equilibrium one. As a consequence of the latter effect, the driving force in the initial stages of film thinning is higher and the drainage is faster.

The increase of τ_{DR} with surfactant concentration in the intermediate concentration range is related to the faster surfactant adsorption, which leads to faster decrease in interfacial tension, which in its own turn leads to slower film thinning. The drainage time at high surfactant concentrations of Span 80 in hexadecane is between 600 and 800 s, which is again in a very good agreement with the value estimated by Eq. (9) for these surfactant concentrations. Also in good agreement are the results determined for τ_{DR} of hexadecane films, containing 0.1 wt% Span 80 with 0 mM NaCl and 500 mM NaCl where Eq. (9) predicts 400 s and 720 s, respectively, with the experimental values falling in the same range, see Fig. 9B above.

However, we cannot explain the results obtained at 1 wt% Span 80 and 500 mM NaCl with the same approach. For this system, the calculated drainage time should be ≈860 s, according to Eq. (9), while we observed that these films remained very thick for more than 3600 s. This unexpected observation could be explained only as being due to formation of non-equilibrium oil films, due to a certain mass transfer between the aqueous and oily phases. Indeed, previous studies with aqueous emulsion films showed that the mass transfer of surfactant, initially dissolved in one of the phases, could lead to non-equilibrium thick films due to Marangoni or osmotic effects which appear when the surfactant is initially dissolved in one of the phases and is transferred slowly into the other phase across the film surfaces [49,50].

To check whether such mass transfer is operative for the systems studied here, we performed additional experiments with oily and aqueous phases which were pre-equilibrated in contact for 1 night. The obtained results from the surface tension and the behavior of the oily films are illustrated in Fig. 11. One sees that the kinetics of interfacial tension is much faster after saturation, as compared to the non-saturated phases. Interestingly the equilibrium interfacial tension measured for the saturated phases is higher, as compared to the non-saturated ones, which is most probably due to exhaustion of the oily phase by some water-soluble components which transfer to the aqueous phase during the equilibration stage. The films formed from pre-equilibrated phases (1 wt% Span 80 in hexadecane and 500 mM NaCl in water) drain to h_{CR} much faster as compared to the non-equilibrated phases (for which no black spot is formed for more than 1 h). After black spot formation, very rapid film rupture is observed within 30–45 s for the equilibrated phases. For films formed from unsaturated phases we cannot determine the film stability because no black spots are formed, but the stability of the saturated phases is very close to the stability of unsaturated phases at lower Span 80 concentration of 0.1 wt%, see Fig. 9C.

From these experiments we conclude that the very long drainage time for 1 wt% Span 80 in presence of 500 mM NaCl is certainly related to a mass transfer from one of the phases to the other phase. As mentioned above, similar phenomenon was observed previously with aqueous emulsion films, formed between two xylene phases and stabilized by the non-ionic surfactant Tween 20 or Tween 80, which had been dissolved initially in the aqueous phase, but has some solubility in xylene as well [49]. This process, called “cyclic dimpling”, is driven by the depletion of the surfactant concentration on the film surfaces due to its dissolution in the oily phase. The depletion triggers a surface convection along the two film surface (Marangoni effect) which drags water towards the film interior and, thus, keeps the film much thicker than its equilibrium thickness [50].

To check what could be the chemical species which could trigger such a mechanism in our system, we performed GC analysis of the studied Span 80 surfactant which is a technical product and contains many components. From the chromatogram shown in Fig. 12 one sees that the used Span 80 sample is rather complex in composition and contains sorbitan monoesters, diesters and triesters, as well as some free fatty acids, sorbitan and isosorbides, which are water soluble. Some of these are water soluble components which may adsorb on the film surface and transfer into the aqueous phase, surrounding the oily film, thus triggering a Marnagoni effect and the related appearance of non-equilibrium emulsion films, as observed experimentally. Alternatively, one may assume a transfer of water molecules into the oily phase where the water may be solubilized in the surfactant micelles, thus forming reverse (W/O) swollen micelles. Such a process would certainly change the chemical potential of the surfactant components in the Span solution, thus affecting the kinetics of adsorption and the equilibrium surface tension, as observed experimentally. Without further systematic study, it would be difficult to clarify which are the exact components responsible for the observed non-equilibrium phenomenon, including the important effect of the NaCl of high concentration (500 mM) needed to observe it.

At the end of this discussion we note that stable equilibrium films, with thickness $h < 10$ nm, is achieved only at very high surfactant concentrations, $C_S > 30$ CMC. These ultrathin films should be stabilized by a steric repulsion between the tails of the adsorbed surfactant molecules on the two opposite film surfaces. Having in mind the very high and comparable concentration of sorbitan mono-, di- and tri-esters in the Span 80 sample used, see Fig. 12, the higher equilibrium interfacial tension and the related lower film stability of the films formed from pre-equilibrated phases, it remains unclear what the actual composition of the adsorption layer is. Thus, it remains unclear which of the Span components is most essential for the film stabilization or, alternatively, some synergistic action is needed, e.g. for formation of a mixed adsorption layer, sufficiently dense to stabilize the film by steric repulsion. It is

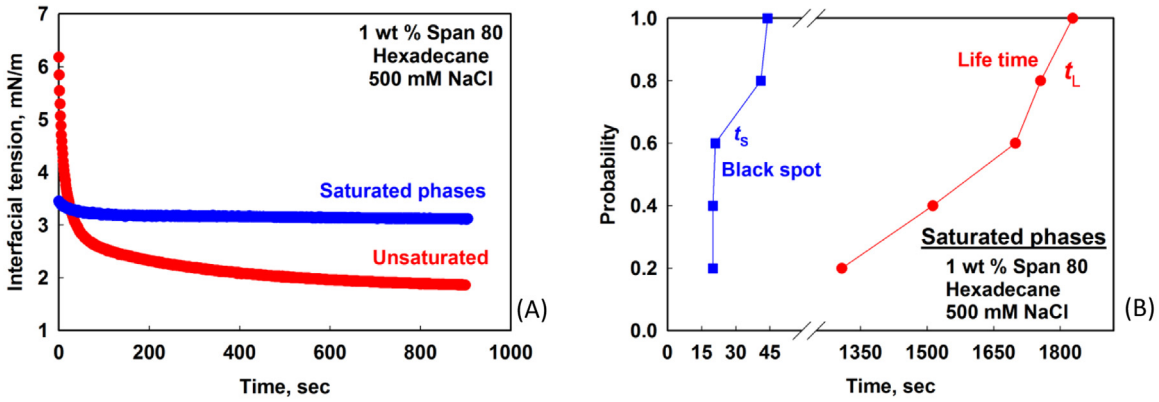

Fig. 11. (A) Interfacial tension for 1 wt% Span 80 in hexadecane against water phase containing 500 mM NaCl measured as function of time for saturated and unsaturated phases; (B) Life time of oily film (red circles) and life time after black spot formation in its interior (blue squares) for films formed from saturated surfaces. (For interpretation of the references to colour in this figure legend, the reader is referred to the web version of this article.)

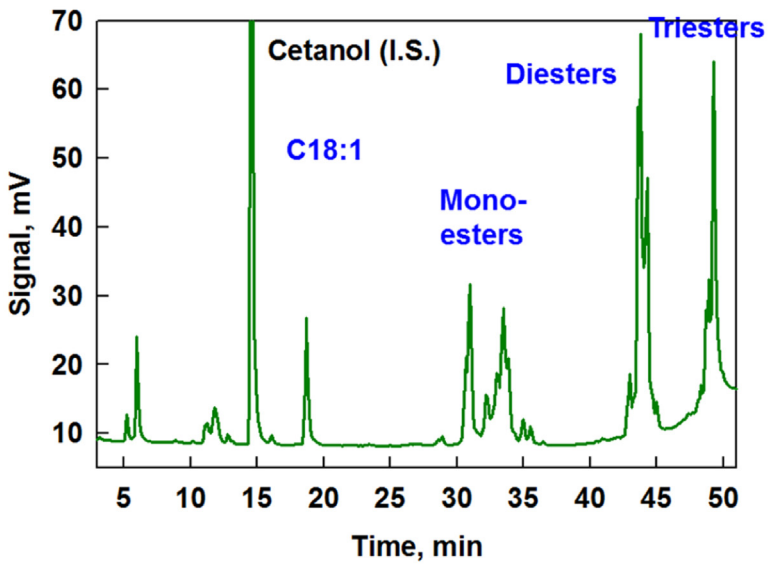

Component	wt. %
Monoesters	30
Diesters	37
Triesters	22
FFA	5
Sorbitan (?)	3
Isosorbides (?)	3

FA content (after hydrolysis)	%
Oleic acid	71
Linoleic acid	22
Palmitic acid	6

Fig. 12. Chromatogram from analysis of used Span 80.

certain, however, that the stability of these thin emulsion films does not correlate with the surface viscoelasticity (viz. with the surface modulus) of the surfactant adsorption layers. Further systematic studies are needed to answer these questions and to analyze the link between the stability of the emulsion films, like those studied here, and the stability of the respective emulsions.

5. Conclusions

The surface properties and the behavior of oily films, formed from hexadecane or Isopar V alkane phase between two aqueous phases, are studied. The concentrations of the nonionic oil-soluble surfactant Span 80 in the alkane phase and of NaCl in the aqueous phase are varied in a wide range. The obtained main results and conclusions could be summarized as follows:

(1) Span 80 forms dense adsorption layers with area-per-molecule of ≈0.30 nm^2, around and above the critical micelle concentration (CMC).
(2) CMC and the main characteristics of Span 80 adsorption layers (such as area-per-molecule and adsorption energy) do not depend on the NaCl concentration in the aqueous phase.
(3) When Isopar is used as oily phase, instead of hexadecane, the CMC is slightly higher and the adsorption energy is slightly lower, while the area-per-molecule is very similar, when compared to those measured with hexadecane.
(4) Interfacial dilatational modulus decreases rapidly with the increase of Span concentration. This modulus does not depend on NaCl concentration in the aqueous phase.
(5) The lifetime of the oily films at concentration up to 10 times CMC coincides with the drainage time of the film, $\tau_L \approx \tau_{DR}$, because the films rupture immediately after the formation of a thin black spot. Such spots are formed at the critical film thickness, $h_{CR} \approx 45 \pm 5$ nm, when the van der Waals forces between the film surfaces become sufficiently strong.
(6) The drainage time increases significantly with the Span concentration, due to the faster surfactant adsorption which leads to lower interfacial tension and, hence, to lower driving force for film thinning. This dependence is described very well by a theoretical model which accounts for both the inhomoge-

neous film thickness and the kinetics of surfactant adsorption along the process of film thinning.

(7) At high Span concentrations, close to 1 wt%, the film life-time increases further, due to the longer life-time of the black films with thickness <10 nm. Some of these films remain stable for more than 30 min. The stability of these thin films is ensured by steric repulsion between the tails of the surfactant molecules, adsorbed on the two film surfaces.

(8) At high Span 80 concentration (1 wt%) and high NaCl concentration (500 mM), the films formed from non-prequilibrated oily and aqueous phases remain with thickness >200 nm for more than 1 h. This effect is explained with the mass transfer of components between the two phases which leads to significant non-equilibrium effects. Comparative experiments with pre-equilibrated oil and water phases resulted in much faster film drainage and rapid film rupture after black spot formation.

(9) The films, formed from Isopar V, are more stable than the films formed from hexadecane solutions, at intermediate and high Span 80 concentrations, due to the longer drainage time. This effect is related to the higher Isopar viscosity.

(10) No correlation is seen between the emulsion film stability and the interfacial viscoelasticity (viz. with the surface modulus) of the surfactant adsorption layers. The film stability increases while the surface modulus decreases rapidly with the increase of Span concentration, due to the faster surfactant adsorption.

The latter conclusion is particularly important, as it is in an apparent contradiction with the conclusions of other studies in this area [30,31]. Further studies are needed to clarify for which types of emulsion the interfacial rheological properties are really important and for which other systems the surface forces (such as steric, van der Waals, etc.) are prevailing.

Acknowledgments

The authors are especially grateful to Ms. Sonia Tsibranska (Sofia University) for performing some of the measurements and for the useful discussions. This study falls under the umbrella of European network COST MP 1305. The authors gratefully acknowledge the support from the Horizon 2020 project ID: 692146-H2020-eu.4.b “Materials Networking”.

References

[1] K.J. Lissant, Emulsions and Emulsion Technology, Marcel Dekker, New York, 1974.
[2] J. Sjoblom, Encyclopedic Handbook of Emulsion Technology, Marcel Dekker, New York, 2001.
[3] P. Becher, Emulsions: Theory and Practice, second ed., Reinhold, New York, 1965.
[4] J. Bibette, F. Leal-Calderon, V. Schmitte, P. Pouline, Introduction in Emulsion Science: Basic Principles, Springer, New York, 2002.
[5] T.G. Mason, J. Bibette, Emulsification in viscoelastic media, Phys. Rev. Lett. 77 (1996) 3481.
[6] T.G. Mason, J. Bibette, Shear rupturing of droplets in complex fluids, Langmuir 13 (1997) 4600.
[7] J.T. Davies, Drop sizes of emulsions related to turbulent energy dissipation rates, Chem. Eng. Sci. 40 (1985) 839.
[8] N. Vankova, S. Tcholakova, N.D. Denkov, I.B. Ivanov, V. Vulchev, T. Danner, Emulsification in turbulent flow 1. Mean and maximum drop diameters in inertial and viscous regimes, J. Colloid Interface Sci. 312 (2007) 363.
[9] A. Sanfeld, A. Steinchen, Emulsions stability, from dilute to dense emulsions — Role of drops deformation, Adv. Colloid Interface Sci. 140 (2008) 1–65.
[10] F.Y. Ushikubo, R.L. Cunha, Stability mechanisms of liquid water-in-oil emulsions, Food Hydrocoll. 34 (2014) 145–153.
[11] S. Tcholakova, N.D. Denkov, A. Lips, Comparison of solid particles, globular proteins and surfactants as emulsifiers, Phys. Chem. Chem. Phys. 10 (2008) 1608–1627.
[12] E. Dickinson, Milk protein interfacial layers and the relationship to emulsion stability and rheology, Colloids Surf. B: Biointerfaces 20 (2001) 197–210.
[13] T.D. Dimitrova, F. Leal-Calderon, T.D. Gurkov, B. Campbell, Surface forces in model oil-in-water emulsions stabilized by proteins, Adv. Colloid Interface Sci. 108–109 (2004) 73–86.
[14] I.B. Ivanov, K.D. Danov, P.A. Kralchevsky, Flocculation and coalescence of micron-size emulsion droplets, Coll. Surf. A 152 (1999) 161–182.
[15] D. Langevin, Influence of interfacial rheology on foam and emulsion properties, Adv. Colloid Interface Sci. 88 (2000) 209–222.
[16] D. Georgieva, V. Schmitt, F. Leal-Calderon, D. Langevin, On the possible role of surface elasticity in emulsion stability, Langmuir 25 (2009) 5565–5573.
[17] E.J. Ekott, E.J. Akpabio, A review of water-in-crude oil emulsion stability, destabilization and interfacial rheology, J. Eng. Appl. Sci. 5 (2010) 447–452.
[18] S. Kokal, Crude-Oil emulsions: a state-Of-The-Art review, SPE Prod. Facil. 20 (2005) 5–12.
[19] T.J. Jones, E.L. Neustadter, K.P. Wittingham, Water-in-crude-oil emulsion stability and emulsion destabilization by chemical demulsifiers, J. Can. Pet. Technol. 17 (1978) 100–108.
[20] J.E. Strassner, Effect of pH on interfacial films and stability of crude oil/water emulsions, J. Pet. Technol. 20 (1968) 303–312.
[21] R. Mohammed Abd, A.H. Nour, A.Z. Sulaiman, Stability of water-in-crude oil emulsion using cocamide surfactant, J. Appl. Sci. 14 (2014) 3270–3275.
[22] Z. Yan, J.A.W. Elliott, J.H.J. Masliyah, Roles of various bitumen components in the stability of water-in- diluted-bitumen emulsions, J. Colloid Interface Sci. 220 (1999) 329–337.
[23] H.W. Yarranton, H. Hussein, J.H. Masliyah, Water-in-hydrocarbon emulsions stabilized by asphaltenes at low concentrations, J. Colloid Interface Sci. 228 (2000) 52–63.
[24] O.V. Gafonova, H.W. Yarranton, The stabilization of water-in-hydrocarbon emulsions by asphaltenes and resins, J. Colloid Interface Sci. 241 (2001) 469–478.
[25] J.D. McLean, P.K. Kilpatrick, Effects of asphaltene solvency on stability of water-in-crude-oil emulsions, J. Colloid Interface Sci. 189 (1997) 242–253.
[26] S. Singh, J.D. McLean, P.K. Kilpatrick, Fused ring aromatic solvency in destabilizing water-in-asphaltene-heptane-toluene emulsions, J. Dispers. Sci. Technol. 20 (1999) 279–293.
[27] T. Dabros, A. Yeung, J. Masliyah, J. Czarnecki, Emulsification through area contraction, J. Colloid Interface Sci. 210 (1999) 222–224.
[28] P.M. Spiecker, P.K. Kilpatrick, Interfacial rheology of petroleum asphaltenes at the oil-water interface, Langmuir 20 (2004) 4022–4032.
[29] P. Tchoukov, F. Yang, Z. Xu, T. Dabros, J. Czarnecki, J. Sjöblom, Role of asphaltenes in stabilizing thin liquid emulsion films, Langmuir 30 (2014) 3024–3033.
[30] W. Albers, J.Th.G. Overbeek, Stability of emulsions of water in oil: I. The correlation between electrokinetic potential and stability, J. Colloid Sci. 14 (1959) 501–509.
[31] F.O. Opawale, D.J. Burgess, Influence of interfacial properties of lipophilic surfactants on water-in-oil emulsion stability, J. Colloid Interface Sci. 197 (1998) 142–150.
[32] P. Kent, B.R. Saunders, The role of added electrolyte in the stabilization of inverse emulsions, J. Colloid Interface Sci. 242 (2001) 437–442.
[33] F.Y. Ushikubo, R.L. Cunha, Stability mechanisms of liquid water-in-oil emulsions, Food Hydrocoll. 34 (2014) 145–153.
[34] S.D. Taylor, J. Czarnecki, J. Masliyah, Disjoining pressure isotherms of water-in-bitumen emulsion films, J. Colloid Interface Sci. 252 (2002) 149–160.
[35] Khr. Khristov, S.D. Taylor, J. Czarnecki, J. Masliyah, Thin liquid film technique — application to water–oil–water bitumen emulsion films, Collids Surf. A: Physiochem. Eng. Asp. 174 (2000) 183–196.
[36] A.G. Gaonkar, R.P. Borwankar, Competitive adsorption of monoglycerides and lecithin at the vegetable oil-water interface, Colloids Surf. 59 (1991) 331–343.
[37] S.C. Russev, N. Alexandrov, K.G. Marinova, K. Danov, N.D. Denkov, L. Lyutov, V. Vulchev, C. Bilke-Krause, Instrument and methods for surface dilatational rheology measurements, Rev. Sci. Instrum. 79 (2008) 104102.
[38] N.A. Alexandrov, K.G. Marinova, T.D. Gurkov, K.D. Danov, P.A. Kralchevsky, S.D. Stoyanov, T.B.J. Blijdenstein, L.N. Arnaudov, E.G. Pelan, A. Lips, Interfacial layers from the protein HFBII hydrophobin: dynamic surface tension: dilatational elasticity and relaxation times, J. Colloid Interface Sci. 376 (2012) 296–306.
[39] R.D. Stanimirova, K.G. Marinova, K.D. Danov, P.A. Kralchevsky, E.S. Basheva, S.D. Stoyanov, E.G. Pelan, Competitive adsorption of the protein hydrophobin and an ionicsurfactant: parallel vs sequential adsorption and dilatational rheology, Colloids Surf. A: Physicochem. Eng. Asp. 457 (2014) 307–317.
[40] A. Scheludko, D. Exerowa, Device for interferometric measurement of the thickness of microscopic foam films, CR Acad. Bulg. Sci. 7 (1959) 123–132.
[41] A. Sheludko, Thin liquid films, Adv. Colloid Interface Sci. 1 (1967) 391–464.
[42] C. Paquot, Standard methods for the analysis of oils, fats and derivatives, Pure Appl. Chem. 53 (1981) 783–794.
[43] P.A. Kralchevsky, K.D. Danov, N.D. Denkov, Chemical physics of colloid systems and interfaces, in: K.S. Birdi (Ed.), Handbook of Surface and Colloid Chemistry, CRC Press, New York, 2008.
[44] A.W. Adamson, A.P. Gast, Physical Chemistry of Surfaces, sixth ed., Wiley, New York, 1997.
[45] L. Peltonen, J. Hirvonen, J. Yliruusi, The behavior of sorbitan surfactants at the water-oil interface: straight-chained hydrocarbons from pentane to dodecane as an oil phase, J. Colloid Interface Sci. 240 (2001) 272–276.
[46] F.O. Opawale, D.J. Burgess, Influence of interfacial properties of lipophilic surfactants on water-in-oil emulsion stability, J. Colloid Interface Sci. 197 (1998) 142–150.

[47] E. Manev, R. Tsekov, R.B. Radoev, Effect of thickness non-homogeneity on the kinetic behavior of microscopic foam film, J. Dispers. Sci. Technol. 18 (1997) 769–788.
[48] B.V. Toshev, I.B. Ivanov, Thermodynamics of thin liquid films – I. Basic relations and conditions of equilibrium, Colloid Polym. Sci. 253 (1975) 558–565.
[49] O.D. Velev, T.D. Gurkov, R.P. Borwankar, Spontaneous cyclic dimpling in emulsion films due to mass transfer between the phases, J. Colloid Interface Sci. 159 (1993) 497–501.
[50] K.D. Danov, T.D. Gurkov, T. Dimitrova, I.B. Ivanov, D. Smith, Hydrodynamic theory for spontaneously growing dimple in emulsion films with mass transfer, J. Colloid Interface Sci. 188 (1997) 313–324.